Carbohydrate Polymers 291 (2022) 119523

Contents lists available at ScienceDirect

Carbohydrate Polymers

journal homepage: www.elsevier.com/locate/carbpol

Effect of gelatinization and swelling degree on the lubrication behavior of starch suspensions

Lei Ji [a], He Zhang [a], Leonardo Cornacchia [b], Guido Sala [a], Elke Scholten [a,*]

[a] Wageningen University, Agrotechnology & Food Sciences Group, Laboratory of Physics and Physical Chemistry of Foods, P.O. Box 17, 6700 AA Wageningen, the Netherlands
[b] Danone Nutricia Research, Uppsalalaan 12, 3584 CT Utrecht, the Netherlands

ARTICLE INFO

Keywords:
Starch tribology
Friction coefficient
Particle properties
Granule morphology
Swelling capacity
Amylose content
Saliva

ABSTRACT

This research aimed to investigate the effect of starch gelatinization and swelling degree on the lubrication properties of starch aqueous suspensions. Three types of maize starch with different amylose content of 70% (HAS), 25% (NS), and <1% (WS) were used to vary the swelling capacities. The granule suspension of NS showed the highest swelling factor (SF) of 26.5, and gave the best lubrication capacity by decreasing friction by 78%. WS was only able to decrease friction by 50% due to a lower swelling capacity. The leached-out amylose increased friction of highly swollen granules (SF = 26.5) but decreased friction of stiff granules (SF = 2.5). Adding unstimulated human saliva to starch suspensions with native and limited swollen granules reduced friction and masked differences in friction coefficients among starch types. Both the salivary layer on the contact surfaces and the salivary proteins in the bulk phase played a role in determining lubrication properties.

1. Introduction

Starch is one of the most abundant polysaccharides in cereals and roots, and is widely used in the food industry as an energy source and as a thickener and fat replacer (BeMiller, 2011; Malinski et al., 2003; Mason, 2009). Due to the capacity to swell upon water absorption and heating, starch suspensions can efficiently increase viscosity (Wang & Copeland, 2013). Starch granules are characterized by semi-crystalline and amorphous concentric layers, mainly due to the presence of amylopectin, which constitutes the backbone of the semi-crystalline structure (Lourdin et al., 2015; Oates, 1997). The other polysaccharide present in starch granules, amylose, is randomly dispersed throughout the amylopectin backbone in both crystalline and amorphous regions. Upon hydrothermal processing (gelatinization), water first enters the amorphous area, and then it diffuses into the crystalline regions, disrupting the crystalline structure irreversibly (Jenkins & Donald, 1998). Due to particle swelling, amylose molecules are able to leach out of the granules, thereby increasing the viscosity of the continuous phase of the starch suspension. The physical properties of starch suspensions thus depend on the properties of both the dispersed starch granules and the continuous phase containing amylose (Debet & Gidley, 2007; Lund & Lorenz, 1984).

The swelling capacity of the granules and the final properties of the starch suspension are related to the amylose/amylopectin ratio (Debet & Gidley, 2006). It is known that a higher amount of amylose reduces the swelling of starch, as amylose double helices require a higher temperature to become disordered compared to the crystalline structures of amylopectin. High-amylose starch therefore shows less swelling ability, and subsequently, a relatively lower amount of amylose leaches out of the granules. For this type of starch, the ratio of leached-out/total amylose can be lower than that of normal starch (Chen & Stokes, 2012; Debet & Gidley, 2006). On the other hand, starches with limited amylose content such as maize waxy starch (amylose <1%), are more prone to swelling (Singh et al., 2014). Thus, the swelling degree of starch granules and the amount of amylose in the continuous phase are very much dependent on the type of starch. The characteristics of starch suspensions can potentially affect the mouthfeel of food products (Chen & Stokes, 2012). Although viscosity plays a role in determining mouthfeel, the tribological properties also influence the mouthfeel to a great extent (Nguyen et al., 2017; Zinoviadou et al., 2008).

Tribology has raised interest in food science as a relevant in-vitro technique to better understand the link between food structure and sensory perception, since rheological properties alone are insufficient to explain some complex mouthfeel attributes such as smoothness,

* Corresponding author.
E-mail address: elke.scholten@wur.nl (E. Scholten).

https://doi.org/10.1016/j.carbpol.2022.119523
Received 26 January 2022; Received in revised form 20 April 2022; Accepted 21 April 2022
Available online 26 April 2022

slipperiness and creaminess (Chojnicka et al., 2008; de Vicente et al., 2006; Kokini et al., 1977; Sonne et al., 2014). It has been proposed that during oral processing, food perception is first dominated by rheology and later by tribology (Stokes et al., 2013). Lubrication behavior is classically presented as a Stribeck curve including three different regimes: the boundary, mixed and hydrodynamic regime (Shewan et al., 2020). The three regimes are often observed for simple viscous fluids. However, in the case of particle suspensions, including suspensions of starch granules, protein aggregates or microgel particles, several deviations from the typical Stribeck curve have been reported (Cassin et al., 2001; Liu et al., 2016; Sarkar et al., 2017; Zhang et al., 2017). Multiple regimes are found as a result of a combination of particle and viscous film lubrication. The lubrication behavior of suspensions is thus dependent on both the properties of the dispersed particles, and the properties of the continuous phase (Chen & Stokes, 2012).

Even though starch is widely applied in many food systems, there are only a few works dealing with its tribological properties. The swelling degree and the irregular shapes of these starch particles are important features for starch suspensions. It is known that spherical particles can improve lubrication of dispersions (Alazemi et al., 2020). It has been shown that larger and stiffer spherical particles provide better lubrication, as they are able to better separate the two opposing surfaces, thereby limiting direct surface-surface contact (Rudge et al., 2020). Besides particle size, shape has also been demonstrated to influence lubrication. Irregularly shaped particles could provide interlocking events among particles and between particles and asperities of the substrate surfaces, thereby increasing friction (Chojnicka et al., 2008; Hafez et al., 2021; Hwang et al., 2011; Wu et al., 2007). The lubrication properties of particle suspensions are thus dependent on particle properties such as size, shape, and mechanical stability. These effects have also been shown for starch systems. For example, it has been shown that starch suspensions, due to the presence of granules, are more efficient in reducing friction than neutral polysaccharides such as locust bean gum and amylose (Zhang et al., 2017; Zinoviadou et al., 2008). In addition, Liu and co-workers showed that a higher number of native rice starch granules with irregular shapes provided high friction (Liu et al., 2016; Zhang et al., 2017). On the other hand, high content of swollen granules with high mechanical stability, which did not disrupt during tribological measurement, led to low friction (Zhang et al., 2017). Besides the starch particles themselves, the amylose in the continuous phase can also affect the lubrication properties. The dissolved amylose was found to improve the lubrication of starch suspensions between roughened substrates (Yakubov, Branfield, et al., 2015; Yakubov, Zhong, et al., 2015). Therefore, many factors could have an impact on the lubrication properties of starch systems.

Gelatinization and swelling are crucial properties of starch suspensions. At the moment, it is not precisely known how these characteristics affect lubrication, which has been linked to sensory attributes affecting the acceptability and palatability of foods (Nguyen et al., 2017; Stokes, 2011; Stribiţcaia et al., 2020; Upadhyay et al., 2020). Therefore, a better understanding of the effect of gelatinization and swelling of starch granules on lubrication might lead to a better control of the quality of starch-containing foods and provides opportunities to alter specific sensory characteristics. To gain more insight into starch lubrication, a systematic investigation of the role of different properties, such as degree of gelatinization, swelling degree, granule size and shape, and degree of leached out amylose, is needed. Therefore, our work focused on the effect of these parameters on lubrication behavior. To change the properties of interest, three types of maize starch were selected with different amylose content: high-amylose (70% amylose), normal (25% amylose), and waxy starch (<1% amylose). Due to differences in crystalline structure and water absorption capabilities, these starches were expected to vary in their granule swelling capacity and amount of amylose leached out in the continuous phase.

2. Materials and methods

2.1. Materials

Three types of maize starch (Hylon 7, Maize starch, Amioca powder TF) with different amylose content were kindly provided by Ingredion Germany GmbH (Hamburg, Germany). The amylose and moisture content of the three types of starch are shown in Table 1. Potassium iodide and iodine were purchased from Sigma-Aldrich Chemie GmbH (Steinheim, Germany). All materials were used without further purification. All samples were prepared with demineralized water (Milli-Q).

2.2. Sample preparation

2.2.1. Preparation of starch suspensions

A stock maize starch suspension with an ingredient concentration of 4% (w/w) was prepared by dispersing starch powder in Milli-Q water for 15 min under gentle stirring. Afterwards, the starch suspension was heated in a water bath under stirring to achieve different gelatinization degree (GD). The conditions of the heat treatments are summarized in Table 2. After heating, the starch samples were cooled down in an ice bath to prevent further swelling and then equilibrated to room temperature (20 ± 0.1 °C). In the following sections, native starch refers to starch suspensions that had not undergone a heat treatment.

2.2.2. Preparation of fractions of the starch suspensions

After heat treatment, the swollen granules and the continuous phase were separated following a method described by Zhang et al. (2017) with slight modifications. The gelatinized starch samples were first centrifuged at 3901*g* at 20 °C for 15 min to obtain a pellet of starch granules and a supernatant containing amylose. The supernatant was collected and centrifuged again under the same condition to remove residual starch granules and obtain the continuous phase of amylose which was used for further analysis. The swollen granule pellet was washed by dispersing it in Milli-Q water and centrifuging again to remove any remaining amylose. The washing step was performed twice to minimize the amount of amylose possibly attached to the swollen granules. Afterwards, the pellet was redispersed in the same amount of Milli-Q water of the collected continuous phase to retain the same concentration of granules present in the original starch suspensions. Swollen granules and continuous phases were prepared freshly before each experiment to minimize retrogradation effects. The continuous phase was also used to obtain amylose powder by a freeze-drying process.

2.2.3. Saliva collection

Unstimulated human saliva was used to investigate the effect of starch degradation and saliva addition on the lubrication properties of the studied starch suspensions. Saliva was obtained in the morning from one healthy 24-year-old female who refrained from consuming any food or beverages except water for a period of 2 h before saliva collection. The unstimulated saliva was collected in a 50 ml centrifuge tube precooled at 4 °C and was kept cool in an ice bath during collection. Then, the collected saliva was centrifuged at 10000*g* for 30 min at 4 °C using a Centrifuge Z-383K (Hermle Labortechnik, Wehingen, Germany)

Table 1
Amylose and moisture content of the three types of studied maize starch.

Starch name	Starch type	Code	Amylose content (%)	Moisture content (%)
Hylon 7	High-amylose maize starch	HAS	70	12.3
Maize starch	Normal maize starch	NS	25	12.8
Amioca powder TF	Waxy maize starch	WS	<1	10.5

Table 2
Heating conditions of the studied starch suspensions.

Starch sample	Temperature (°C)	Time (min)
HAS	75, 85, 95, 99	5, 30[a]
NS	65,75, 85, 95	
WS	65,75, 85, 95	

[a] Only used for samples heated at 95 °C.

to remove cellular debris. The supernatant was collected and stored at −80 °C. Before experiments, saliva was defrosted overnight at 4 °C.

2.2.4. Preparation of gelatinized starch and saliva mixtures

Starch-saliva mixtures were incubated in a water bath at 37 °C, which is comparable to the human oral temperature. Prior to mixing, starch samples and saliva were put into the water bath separately for 2 min for temperature equilibration. Afterwards, they were mixed in a plastic tube (50 ml) in a ratio of starch: saliva of 9:1 (w/w). This amount of saliva was determined by a "sip and spit" test, and the average saliva incorporated was determined (data not shown). The incubation time ranged from 30 min to 18 h at 37 °C to follow the hydrolysis process of the starch granules. After incubation, the mixture was cooled down fast in an ice bath and equilibrated to room temperature (20 ± 0.1 °C). Subsequently, the microstructure of the samples was visualized under a microscope.

2.3. Sample characterization

2.3.1. Particle size determination and swelling degree calculation of granules

The particle size distribution of the samples was measured by static light scattering with a MasterSizer (MasterSizer2000, Malvern Instruments Ltd., Malvern, UK). The refractive index of water was set to 1.33 and the particle size was reported as volume weighted mean (D[4,3]). All the measurements were performed in triplicate and particle size is presented as mean ± standard deviation.

The volume of the native and swollen granules was estimated from the measured size (D[4,3]) assuming the particles to be completely spherical. The swelling degree of the granules presented in this work as swelling factor (SF) was then calculated based on the volume of the swollen particles ($V_{swollen}$) and the initial volume of the native particle (V_0) as

$$SF = V_{swollen}/V_0 \quad (1)$$

2.3.2. Dry mater determination of leached-out amylose phase

The separated continuous phase was collected and placed in an oven at 105 °C overnight to determine its dry matter. All the measurements were performed in triplicate. The weight of leached-out amylose (dry mass, $g_{amylose}$) was divided by the weight of the used starch powder (dry mass, g_{starch}) to obtain the ratio of leached-out amylose to total starch dry matter ($g_{amylose}/g_{starch}$). Afterward, a leaching efficiency (in %) was calculated based on the original total amount of amylose in the granules, which was 25% for NS and 70% for HAS.

2.3.3. Light microscopy

The starch granules were visualized using a Zeiss Axio light microscope (AxioSkop 2 plus, Carl Zeiss GMBH, Oberkochen, Germany). Native and gelatinized starch samples were diluted 4 and 10 times, and then stained with a 0.2% iodine solution (I2: 2 g/l; KI: 20 g/l). The images were magnified 20 and 50 times.

To evaluate the crystalline nature of the starch granules, birefringence of starch granules was observed using a Zeiss Axio light microscope equipped with two crossed polarized filters. An objective of 50× was used. All digital images were obtained by a camera (AxioCam ERc 5 s, Zeiss, Oberkochen, Germany) attached to the microscope.

2.3.4. Differential Scanning Calorimetry (DSC)

The thermal behavior of starch suspensions was determined with a thermal analyzer (DSC 25, TA instruments, Inc., Philadelphia, US). Approximately 40 mg of the starch suspensions were weighed into a stainless-steel high volume pan and hermetically sealed, and then transferred to the DSC autosampler. Milli-Q water sealed in the same type of pan was measured as a reference. The samples were first equilibrated at 20 °C for 5 min, and then temperature was increased from 20 to 200 °C at a heating rate of 5 °C/min, and subsequently decreased from 200 to 20 °C at a cooling rate of 5 °C/min. The enthalpy of gelatinization (ΔH) from the first run was calculated. Data were collected and analyzed using the software TRIOS (TA Instruments TRIOS). All the measurements were performed in triplicate.

2.3.5. Viscosity measurements

The viscosity of the starch suspensions was measured using a stress-controlled rheometer (MCR 302, Anton Paar, Austria) with a double gap geometry (probe DG.26.7/Ti; cup DG 26.7/T200/Ti) or a concentric cylinder geometry (probe CC17/Ti; cup CC17/Ti) depending on the consistency of the sample. Samples of either 3.8 ml (double gap) or 4.7 ml (concentric cylinder) were poured into the cup and kept at 20 °C for 5 min before the measurement started. The shear rate was increased in logarithmic steps from 0.1 s^{-1} to 1000 s^{-1} in 5 min and then decreased from 1000 s^{-1} to 0.1 s^{-1} in 5 min. Data points were collected every second. All measurements were performed in triplicate, and the average value of the viscosity (increasing shear rate) was used and plotted as a function of shear rate.

2.3.6. Determination of gelatinization degree (GD)

The degree of gelatinization (GD) was determined by comparing the viscosity of the starch suspensions before and after gelatinization. First, the viscosities (η_0) of native starch (non-heated) suspensions with different starch concentrations (C) (1, 5, 10, 15, 20 and 30%) were measured to obtain a calibration curve (Genovese & Rao, 2003). Then, the viscosity of starch suspensions after heat treatment (η_{heat}) with specific starch concentrations was measured. The calibration curve was used to obtain the corresponding apparent concentration (c_{heat}) of the suspension with swollen granules. The GD was then determined by comparing the apparent concentration of the swollen starch granules suspension to that of the native starch suspension (c_0) as:

$$GD = c_{heat}/c_0 \quad (2)$$

The viscosity increase was the result of both the swelling of the granules and the contribution of the leached out amylose in the continuous phase.

2.3.7. Tribological measurements

Tribological measurements were performed with a stress-controlled rheometer (MCR 302, Anton Paar, Austria) equipped with a tribology accessory (T-PTD 200, BC 12.7, Anton Paar, Austria). A glass-PDMS tribo-pair was employed to mimic the oral cavity: glass was used to mimic the palate and the relatively softer PDMS was used to mimic the tongue, as it can better emulate the elastic properties of this organ (Carpenter et al., 2019; Dresselhuis et al., 2008; Fan et al., 2021; Vlădescu et al., 2021). The set-up was based on a glass ball-on-three-pins principle, consisting of a spherical glass ball (d = 12.7 mm) and three PDMS pins (d = 6 mm, roughness 0.2 μm ± 0.03). A schematic representation of the experimental setup is shown in the supplementary information (Fig. A.1). The temperature was kept at 20 °C and a normal force, $F_{N,}$ of 1 N was applied. Samples with a volume of 0.6 ml were inserted in the tribometer cup, and the friction coefficient was measured as a function of sliding speed. One measurement consisted of 3 runs of 5 min each (15 min in total for one measurement) with increasing, decreasing and increasing sliding speed, v_s, between 0.01 and 470 mm/s. Data points were collected every second. The data of the first run were discarded as the results often deviated among triplicates. The data of the

third run (increasing sliding speed) were selected for further analysis. Each measurement was performed in triplicate with new samples. The averaged value of friction coefficient (μ) was determined as a function of sliding speed.

For samples with saliva addition, the temperature was kept at 37 °C and a normal force, F_N, of 1 N was applied. The friction of the starch suspension was first measured at a constant sliding speed of 1 mm/s for 3 min to obtain a constant friction coefficient. Saliva was then added into the starch sample and the friction coefficient of mixtures was recorded for 4 min until a constant value was obtained. In a further measurement, the friction coefficient of saliva was first recorded at a constant sliding speed of 1 mm/s for 3 min. Saliva with a volume of 0.6 ml was first added to the tribometer cup. The friction coefficient was then measured at a constant sliding speed until a constant value, confirming that a layer of saliva was applied on the PDMS substrate. Excess saliva (0.54 ml) was then removed. Afterwards, the starch samples (0.54 ml) were added and the friction coefficient of the mixtures was recorded for 4 min. The ratio between starch and saliva was kept at 9:1 (starch: saliva, w/w) in both types of measurements.

2.3.8. Saliva protein determination by SDS-PAGE

The protein species in the collected saliva were analyzed by sodium dodecyl sulfate polyacrylamide gel electrophoresis (SDS-PAGE) under non-reducing conditions. Saliva was mixed with diluted (20×) running buffer (NuPAGE MES SDS Running Buffer) and incubated at 70 °C for 10 min. Approximately 5 μl of marker and 20 μl of saliva samples were loaded on a NuPAGE Novex Bis-Tris Gel (NuPAGE, Hercules, California, USA). Then the gel was connected to electrodes set at 200 V until the samples migrated to the end of the gel. All blue pre-stained standard (Precision Plus Protein, Bio-rad Laboratories, Hercules, California, USA) was used as a protein marker with a molecular size range from 2.5 kDa to 200 kDa. The gel was stained by Coomassie blue (InstantBlue, Expedeon, San Diego, USA) and then analyzed by Image Lab software (Bio-rad Laboratories, Hercules, California, USA).

3. Results and discussion

3.1. Gelatinization degree (GD), swelling factor (SF) and particle size distributions

The size of the starch granules was characterized before and after heat treatment. The measured particle size (D[4,3]), and the calculated GD and SF are shown in Table 3. With increasing heating temperature and time, granules swelled to a larger size, and both SF and GD increased, showing that higher heating temperatures or longer heating times induced water absorption and expansion of the granules.

Table 3
Heating conditions, averaged particle size (D [4,3]), gelatinization degree (GD), and swelling factor (SF) of high-amylose starch (HAS), normal starch (NS), and waxy starch (WS).

Maize starch type	Heating temperature (°C)	Heating time (min)	Averaged particle size (μm, D[4,3])	GD	SF
HAS	–	–	14.3 ± 0.2	1.0	1.0
	75	5	15.8 ± 0.2	2.4	1.3
	85	5	18.4 ± 0.2	2.7	2.1
	95	5	22.5 ± 0.2	3.2	3.9
	99	5	23.4 ± 0.1	5.9	4.4
	95	30	24.3 ± 0.1	6.2	4.9
NS	–	–	15.6 ± 0.2	1.0	1.0
	65	5	21.1 ± 0.1	2.2	2.5
	75	5	28.3 ± 0.1	7.4	6.0
	85	5	33.1 ± 0.2	9.1	9.6
	95	5	41.7 ± 0.1	14.6	19.1
	95	30	46.5 ± 0.1	18.2	26.5
WS	–	–	17.5 ± 0.3	1.0	1.0
	65	5	28.9 ± 0.2	2.8	4.5
	75	5	38.4 ± 0.6	23.9	10.6
	85	5	39.5 ± 0.8	29.4	11.5
	95	5	39.1 ± 0.4	35.0	11.2
	95	30	40.1 ± 0.1	35.0	12.0

To visualize the effect of amylose/amylopectin ratio on swelling behavior, we plotted the SF of the studied starches versus their GD. The increase in SF of NS particles was much greater than that of HAS (Table 3, Fig. 1a). The limited expansion of HAS granules can be explained by the high resistance to swelling of the amylose. As amylose is present as a double helix, it requires a higher energy to achieve a disordered state. This effect prevents fast water binding, which decreases the swelling capacity (Debet & Gidley, 2006).

Compared to HAS and NS, the granules of WS consisted only of amylopectin (>99%), and, therefore, swelled more easily at lower heating temperatures and times (Fig. 1a and Table 3). Their GD increased up to a factor of 35. However, the particle size of WS did not follow this trend. It first increased and then became almost constant at a GD range from 23.9 to 35 (Fig. 1a). The plateau in the swelling degree can be explained by the fact that after swelling to a certain extent (SF ~ 10.6), part of the WS granules were broken down into smaller fragments. The increase in size of the swollen granules was thus compensated by a decrease in size due to granule break down. This effect has also been observed in other studies (de Clerck, 2009). Broken granules or granule fragments still contributed to an increase in viscosity i.e., GD, but did not affect the SD anymore. The presence of smaller granule fragments was confirmed when plotting the particle size distribution as a number fraction (Fig. 1b). For NS and HAS samples, granule fragments were observed neither in microscopy images (Fig. 2a) nor in particle size distribution curves (data not shown). Thus, the granule swelling capacity followed the order: normal starch (NS) > waxy starch (WS) > high-amylose starch (HAS). A schematic representation of starch gelatinization is shown in Fig. 1c.

3.2. Morphology of starch granules with various SF

The morphology of starch granules was characterized using light microscopy, and the obtained images are shown in Fig. 2a. Changes in granule morphology induced by gelatinization were clearly observed for all three types of starches with varying SF. The granules of native starch (1.0) were smaller and polyhedral shaped, with sharp edges. The increase in size of HAS granules with increasing SF was limited, as observed in Fig. 2a, while the volume expansion of the granules after gelatinization was more evident for NS and WS. This was in line with the results obtained for the particle size distribution (Fig. 1 and Table 3). The images of Fig. 2a also confirmed that for WS some of the swollen granules broke down into smaller fragments and lost their integrity. In addition, at a SF of 4.5, the water absorption of different WS granules varied, as some of the granules swelled to a quite large size (~50 μm) or broke, but some granules did not swell and remained present as native starch granules (~20 μm). Once the SF reached 10.6, most granules were swollen, and some swollen granules started to break down into smaller fragments.

Along with the change in size and morphology due to starch gelatinization, the crystalline structure inside the granules was also altered. Before gelatinization, the semi-crystalline layers within the granules could be identified under polarized light as Maltese crosses. Upon gelatinization, the crystalline structure disappeared, and as a result the Maltese crosses also disappeared. The degree of birefringence is a well-known indication of the degree of crystallinity (Pérez et al., 2009). For all three starches, the effect of SD on the presence of the typical Maltese crosses of the starch granules is shown in Fig. 2b. With a higher swelling degree, the birefringence became weaker, indicating the loss of a crystalline structure due to gelatinization (Pérez et al., 2009). However, the extent of structure disruption was clearly different for the three types of starches. For HAS granules, birefringence was still visible at the highest swelling degree of 4.9 (heated at 95 °C for 30 min). The morphology of

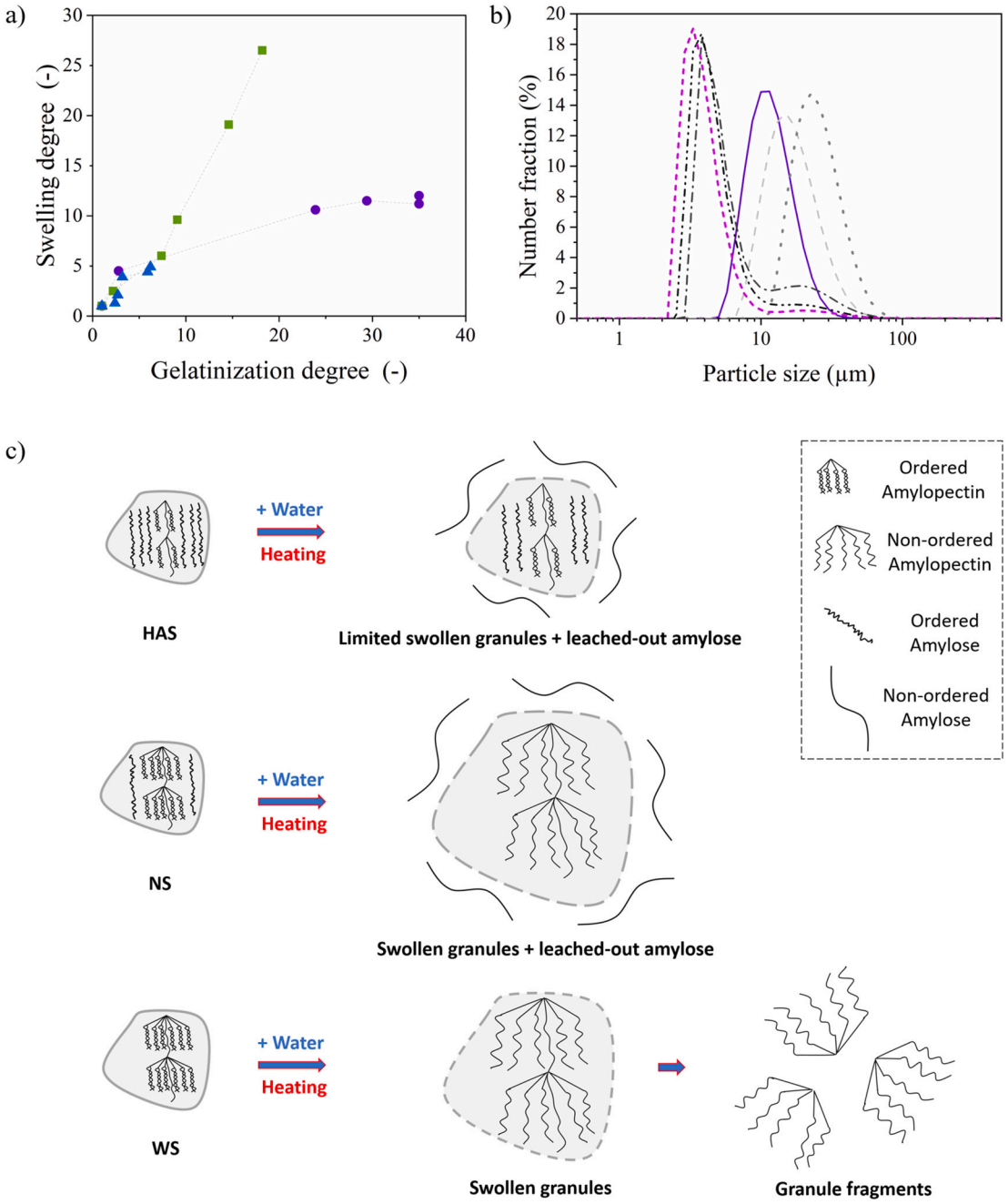

Fig. 1. a) Swelling degree versus gelatinization degree for high-amylose starch (HAS) (blue triangle), normal starch (NS) (green square), and waxy starch (WS) (purple circle). b) Particle size distribution (number fraction) of 4% WS suspensions with different swelling degrees of: 1.0 (purple line), 4.5 (light grey dash line), 10.6 (grey dot line), 11.5 (dark grey dash dot line), 11.2 (black dash dot line), and 12.0 (magenta short dash line). c) Schematic representation of starch granule gelatinization for HAS, NS, and WS. The drawing is based on the description of the thermodynamics of starch swelling and gelatinization by Renzetti et al. (2021) and Xu, Blennow, et al. (2020).

the swollen granules also suggests that the gelatinization started at the center region (hilum) and then spread to the periphery of high-amylose granules (Tao et al., 2018). Thus, in this study, HAS granules after gelatinization were expected to be stiff particles as the outer region remained crystalline. HAS would need to be heated to 130–150 °C to achieve complete gelatinization, as shown in DSC experiments (data not shown) and other studies (Macakova et al., 2010; Zhang et al., 2017). In comparison, NS granules lost their crystallinity (Maltese cross) when the SF reached a value of 6.0 (heated at 75 °C for 5 min). For WS, the crystalline pattern disappeared after reaching a SF of 10.6 (heated at 75 °C for 5 min). For waxy maize starch, the disappearance of the crystalline nature of the granules at lower temperatures of 75 °C has been reported in literature (Macakova et al., 2010; Zhang et al., 2017). As a result of the increase in SD and the progressive loss of the internal crystalline structure, the starch granules were expected to become softer and more deformable (Desse et al., 2010). NS and WS starch particles were thus expected to be softer than the HAS particles.

3.3. Lubrication behavior of different starch types

3.3.1. NS suspensions

To discuss the effect of the swelling degree on lubrication properties, we start with NS, since its granules swelled to a large extent without breaking into fragments. The Stribeck curves of NS suspensions, also

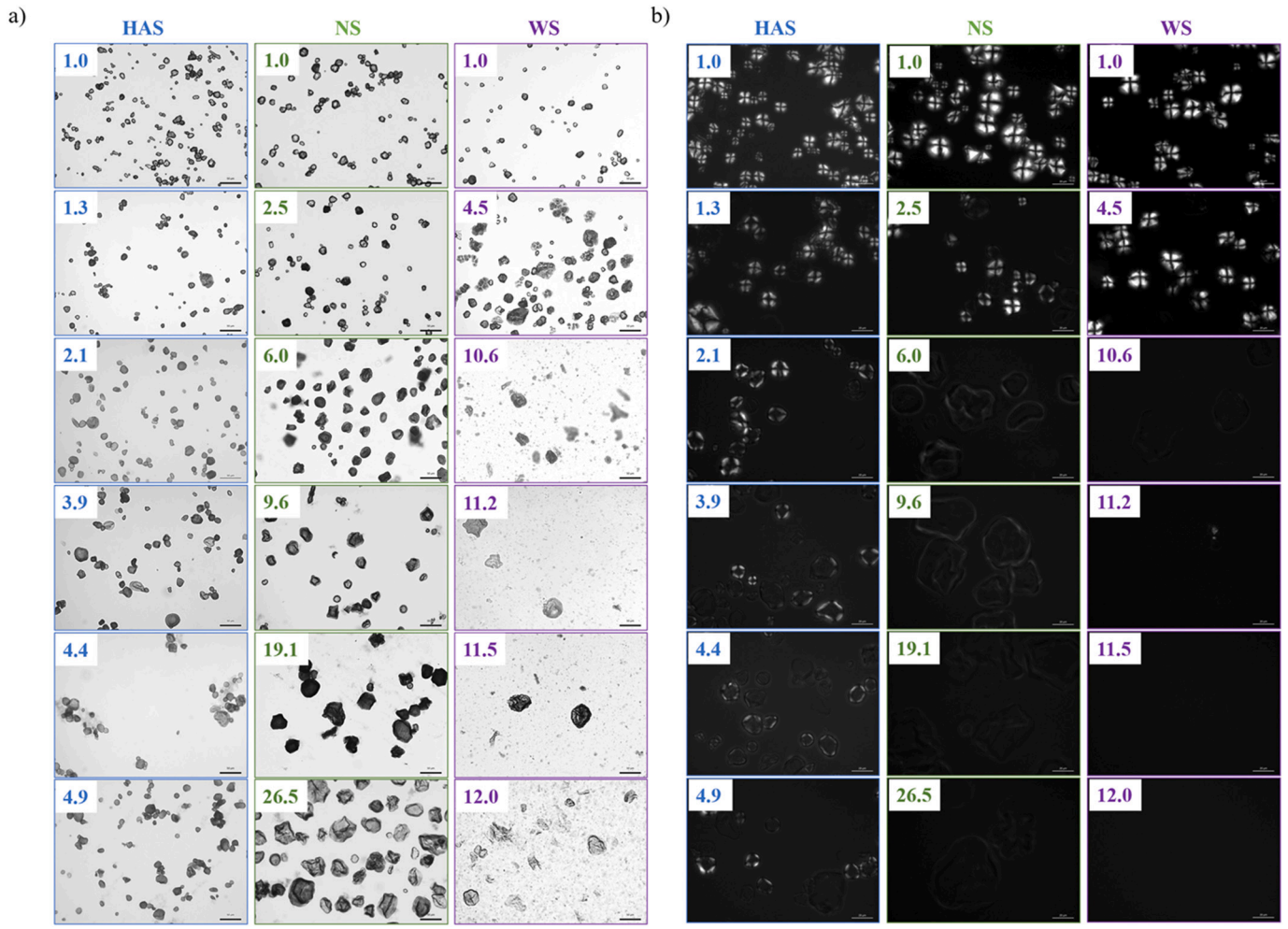

Fig. 2. a) Morphology of starch granules of high-amylose starch (HAS), normal starch (NS), and waxy starch (WS) with different swelling degrees visualized with light microscopy. The scale bar in the figures represents 50 μm. b) Birefringence of starch granules of HAS, NS, and WS with different swelling degrees under a polarized light microscope. The scale bar in the figures represents 20 μm.

those obtained upon normalization for viscosity, are shown in Fig. 3.

The friction behavior of water (dashed grey line) and NS suspensions show that lubrication occurred in the boundary and mixed regimes, and no hydrodynamic regime was observed, indicating that both lubricant and surface (glass and PDMS) properties influenced the lubrication properties. The presence of starch granules led to lower friction. This was most likely due to the motion of the granules, providing lubrication via particle sliding/rolling between the two sliding surfaces. This agrees

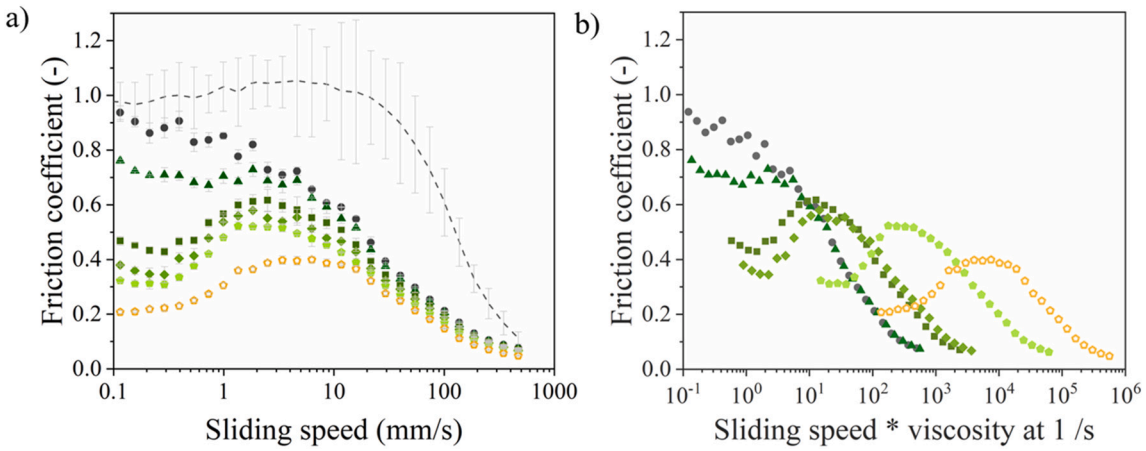

Fig. 3. Friction coefficient as a function of a) sliding speeds and b) the friction parameter (speed * viscosity at 1 s^{-1}) of normal starch (NS) suspensions with various SF: 1.0 (black circle), 2.5 (dark green triangle), 6.0 (green square), 9.6 (green diamond), 19.1 (light green pentagon), and 26.5 (yellow open pentagon). In Fig. 3a, the friction curve of water is added as reference (dashed line).

with the results obtained for other particle-containing systems (Olivares et al., 2019; Rudge et al., 2020; Yakubov, Branfield, et al., 2015; Yakubov, Zhong, et al., 2015; Zhang et al., 2017; Zinoviadou et al., 2008). As shown in Fig. 3a, when the SF increased, the friction coefficient changed to a large extent, especially in the boundary regime. An increase in friction with increasing sliding speed was observed for samples with a SF above 2.5. It is well known that with increasing degree of gelatinization, the viscosity of starch suspensions increases due to an increased volume of the granule phase and to the amylose that leached-out in the continuous phase (Liu et al., 2016; Zhang et al., 2017). Therefore, the effects of viscosity of starch suspensions on frictional behavior were first evaluated. The viscosity data are reported in the supplementary information section (Fig. A.2).

Based on the results of the viscosity measurement, the samples showed either Newtonian (SF $<$ 19.1) or shear-thinning behavior (SF $=$ 19.1 and 26.5), and, therefore, the maximum in the friction curves of the samples could not be explained by shear thickening. One explanation might be that with increasing sliding speeds jamming effects of the particles between the surfaces occurred, which could lead to an increase in friction coefficient. This has also been discussed in other studies with hydrogel particles (Rudge et al., 2020). With a further increase of the sliding speed and subsequent increase in the size of the gap, the jamming effect might be eliminated and the friction coefficient would decrease again. This phenomenon has been observed in other studies on starch (Zhang et al., 2017).

To take a further look at the effect of viscosity on frictional behavior, the viscosity at a shear rate of 1 s^{-1} was taken in consideration to transform the sliding speed into the frictional parameter (sliding speed * viscosity). At all shear rates, the trend was similar (Fig. A.2), but the viscosity at a shear rate of 1 s^{-1} had the largest influence on friction. Therefore, the viscosity at this shear rate was chosen to show the effect of viscosity on friction. As shown in Fig. 3b, after correcting for the viscosity, the friction curves still show a significant difference. If viscosity would dominate the behavior, the curves would be expected to overlap to give a “master curve” (Stokes et al., 2011). However, neither the boundary regime nor the mixed regimes of the friction curves overlapped, indicating that the lubrication behavior was not dominated by viscosity, but depended more on the properties of the particles. This effect is clear when we compare samples with different swelling degree. By comparing the samples with a SF of 6.0 (green square), 9.6 (green diamond), and 19.1 (light green pentagon), we saw that friction in the mixed regime decreased with increasing SF (Fig. 3a). However, the reason for the decrease in friction appeared to be different for the different samples. After multiplying the sliding speed by viscosity, the part of the curves corresponding to the mixed regime of the samples with a SF of 6.0 and 9.6 overlapped, which suggests that the lower friction of the sample with a SF of 9.6 could be explained by viscosity. However, for the sample with a SF of 19.1, the curve did not overlap with the SF 6.0 samples, which shows that for this sample, lubrication was not determined by viscosity only, but that the lubrication properties were more dominated by the particle characteristics.

It is well known that particle properties such as size, deformability, shape, and particle volume fraction are important factors to lubrication (De Wijk & Prinz, 2006). Before we discuss the results of the NS particles, we first highlight the expected effect of these properties. In general, we expect low friction coefficients with limited surface-surface and surface-particle contact, and high friction coefficients with high surface-surface and surface-particle contact. Limited contact area provides a higher rolling ability of the particles, which is known as the ball-bearing mechanism. Low friction coefficients are expected when particles are large and spherical, as they can better separate the two sliding surfaces by increasing the gap size, and thus prevent the direct contact of the surfaces (Rudge et al., 2020; Stribiţcaia et al., 2020). Such direct contact between the sliding surfaces is also limited when particles are present in higher volume fractions (Chojnicka et al., 2008; Rudge et al., 2020; Zhang et al., 2017). Comparing particles with similar size but different deformability, stiff ones are expected to generate low friction coefficients, as they would roll better and thus limit the contact area between the particles and the sliding surfaces (Rudge et al., 2020). Soft and deformable particles can easily deform under the applied normal force, which would induce an increase of the surface-particle contact area, and therefore provide higher friction coefficients. Limited contact area, and accompanying lower friction coefficient, are also expected for particles that are completely spherical. In contrast, for particles with non-spherical shapes, large contact areas between particles and the sliding surfaces and among particles are expected, decreasing their rolling ability, providing higher friction coefficients. In addition, particles with a rough surface could interlock with rough sliding surfaces, which is unfavorable for lubrication. Fig. 4 provides a schematic overview of these effects on particle lubrication in the boundary and mixed regimes, in which the gap size is limited and the interactions between particles and contact surfaces dominate frictional behavior.

These general effects of particle properties have been discussed for model particle suspensions. However, the starch granules in our study always change in more than one parameter. For example, in dispersions with higher GD, particle size increases, while the granules become more deformable, and their shape and surface roughness may change. This complicates the interpretation of the results. As shown in Fig. 3a, the friction coefficient for the NS particles decreased with increasing SF, suggesting that large and deformable particles provided better lubrication than small and stiff particles. As discussed before, it has been shown that if particles are large, low friction coefficients are expected (Rudge et al., 2020; Stribiţcaia et al., 2020). These larger particles were also softer and more deformable. Based on the discussed effect of deformability, we would expect more deformable particles to provide higher friction coefficients, since they have larger particle-surface contact areas. As we see a decrease in friction coefficient for larger and softer particles, it seems that the friction coefficients for the NS particles were more determined by the size than by the deformability of the particles. In addition, the lower friction coefficients may also be explained by the increased volume fraction of the particles due to particle swelling. We must note that also changes in the shape may play a role. In the case of small and hard particles, the sharp edges of the granules could result in more interlocking events with asperities on the surface, which would inhibit particle motion (Hafez et al., 2021). High friction coefficients for irregular particles were also seen in other particle-containing systems such as protein aggregates with irregular shapes (Chojnicka et al., 2008). However, upon swelling, the starch granules may also change their shape under compression. This may reduce interlocking events with the sliding surfaces, positively affecting lubrication. The higher deformability may therefore also lead to a decrease in the friction coefficient for non-spherical particles, opposite of what is discussed for spherical particles. The effect of deformability on particle lubrication for non-spherical particles has been rarely discussed. Although high deformability of spherical particles has been discussed in literature to increase friction, we cannot rule out the fact that high deformability for non-spherical particles could contribute to lower friction. Overall, the lower friction coefficients observed upon swelling may be linked to an increase in size, increase in volume fraction, or to changes in shape due to a higher deformability.

Besides the absolute values of the friction coefficients, the shape of the friction curves for NS with different SF was also different (Fig. 3). For starch suspensions containing granules with higher swelling degrees (SF $>$ 6), the friction coefficient increased first and then decreased with increasing sliding speeds. This behavior has been observed in other soft particle-containing systems (Gabriele et al., 2010; Rudge et al., 2020; Shewan et al., 2020; Zhang et al., 2017) and has been ascribed to the fact that in particle suspensions, shear can cause jamming effects (Bi et al., 2011; Lafond et al., 2013; Wang et al., 2019), thereby increasing the friction coefficient. Such jamming effects can occur when large soft particles try to pass the small gap between two sliding surfaces. When these highly-swollen deformable particles try to enter the gap and once

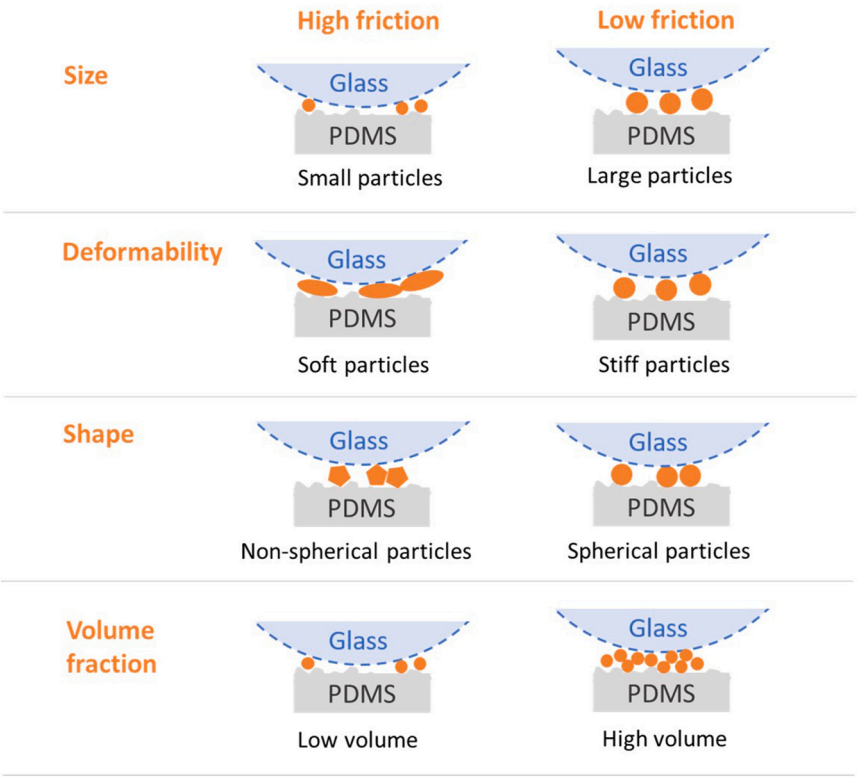

Fig. 4. Schematic presentation of the effect of particle size, deformability, shape on lubrication properties. The orange items indicate particles.

they have entered the gap, they have more probability to show such jamming effects and therefore increase the friction coefficient (Rudge et al., 2020; Zhang et al., 2017). Upon an increase in sliding speed, the hydrodynamic pressure between the sliding surfaces increases, enlarges the gap size, which reduces the jamming events and thus decreases friction again.

To evaluate the effect of granule volume fraction, we separated the granule phase and the continuous phase of the suspensions containing the most swollen granules (SF = 26.5) and then diluted the granule phase to different concentrations, i.e. 4%, 0.4%, 0.04%, and 0.01% (data shown in supplementary as Fig. A.3). We observed that the friction coefficients increased with decreasing granule volume fraction, confirming that a high-volume fraction showed a positive effect on lubrication. Additionally, the friction coefficient did not increase with an increasing sliding speed at a low concentration of 0.01%, supporting the hypothesis that the jamming effects disappeared at a low volume fraction. These results also confirmed that good lubrication of highly swollen granules was partly due to the increase in volume fraction.

The results presented above suggest that the changes in particle properties, such as size and deformability/stiffness, and particle volume fraction, were responsible for the changes in lubrication behavior in both boundary and mixed regimes. The results also show that the friction coefficients in the boundary regime were most likely determined more by the size rather than by the deformability of the particles, and that the effect of differences in size was more evident at higher speeds. As size and deformability could not be changed independently, we could not decouple their effects. However, to get more insights in the tribological functionality of the different starches, we compared the results with the behavior of the HAS and WS suspensions.

3.3.2. *HAS and WS suspensions*

In the case of HAS systems, birefringence was observed for all swelling degrees (Fig. 2b). Therefore, these granules were likely stiffer than those present in most NS samples due to their crystalline structure, but their size still changed. The measured friction curves of HAS suspensions with different SF were similar (data shown in supplementary information as Fig. A.4a).

These results indicate that the friction behavior was not altered by increasing particle size i.e. SF. The friction coefficient did not decrease even when the swollen granules were 4.9 times larger than the native granules. One could argue that the change in size was too small to make a difference in lubrication behavior. However, the friction coefficients of NS suspensions already started to decrease when the SF was 2.5. If particle size would be the only factor dominating tribology, the friction coefficient of HAS systems would decrease even at the SF observed for these samples. Therefore, the size itself cannot exhaustively explain the lubrication behavior of the granules. Most likely, the fact that HAS granules remained stiff and irregularly shaped also with increasing SF, as demonstrated by the birefringence of all samples, played an important role. The angular shape and low deformability prevented the particles from moving between the sliding surfaces, and, therefore, generated high friction coefficients.

In the case of waxy starch (WS) suspensions, the granules became much softer as a result of the extensive swelling (data shown in supplementary information as Fig. A.4b). When the SF was high (>4.5), they even broke down into smaller pieces, which limited the increase in SF (Fig. 2a and b). The volume fraction of the granules was high, but the increase in particle size was limited. Noticeably, the curves of WS with SF > 4.5 mostly overlapped (data shown in supplementary information as Fig. A.4b). This is most likely because the size stayed quite similar (38.4–40.1 μm), though these systems varied a lot in particle volume fraction (as GD increased from 23.9 to 35.0). Beyond an SF of 4.5, fragments were present in the starch systems as evidenced in light microscopy in Fig. 2a. The similar friction coefficients are thus most likely explained by the average particle size of the starch suspension. The similar particle size also explains why the increase in the friction coefficient occurred at the same speed, and in a similar fashion.

As mentioned, the effect of gelatinization in the WS system was quite limited, and much smaller than the reduction in friction for the NS system (Fig. 3a). This was probably due to the fact that the friction

coefficients of the native WS system were already much lower than that of the native NS system. Since the native granules were of the same size, this may be due to differences in the particle shape. As the native NS granules provided a higher friction coefficient, and could swell to a large degree, differences in shape may explain the much larger decrease in friction.

To summarize, the friction behavior of starch suspensions depends on the type of starch used, and particle size seems to be the most important factor to influence this behavior. An increase in size leads to larger gap size and lower surface-surface contact, which benefits lubrication. To compare the different starches, we plotted their friction coefficient as a function of SF (Fig. 5). HAS granules were more difficult to swell, and therefore provided the highest friction coefficient after the heating process. Even though native NS gave the highest friction, with increasing particle swelling, the friction coefficient of this starch decreased by 78% and was the lowest at the highest degree of swelling. Though native WS gave the lowest friction and showed the highest GD (Fig. 1a), granule break up limited the variation in lubrication. WS was less efficient in reducing friction and a reduction of 50% only was obtained. Therefore, NS provides a better possibility to control friction, as it has the widest range of swelling degrees and particle sizes. The particle size has a large influence on the gap size to decrease surface-surface contact, which seems to be the most important factor from these results. However, as discussed earlier, the effect of deformability of non-spherical particles is not clear, and may need to be considered.

3.4. Amylose content in the continuous phase

In the previous section, we have only considered the effect of the dispersed starch granules. Another important factor potentially influencing friction is the amylose leaching out from the granules into the continuous phase due to granule swelling. The amount of leached out amylose depends on the amylose content and thus varies with starch type. The amount of amylose that leached out from the granules of HAS and NS is summarized in Table 4.

With increasing GD, an increasing amount of amylose leached out into the continuous phase for both types of starches, which was expected. We found that with comparable GD, such as 2.4 (HAS) and 2.2 (NS), the amount of leached-out amylose was also comparable. As the amylose content of HAS was more than twice that of NS, HAS was less capable to swell. The amount of leached-out amylose seemed to be more related to the degree of swelling than to the initial amylose content in

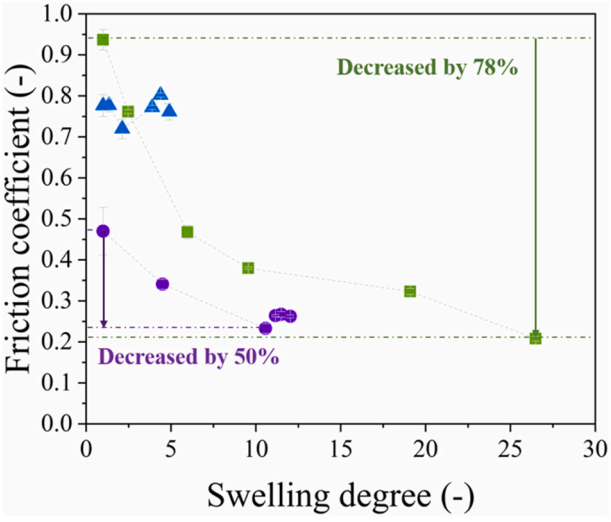

Fig. 5. Friction coefficient at 0.1 mm/s as a function of swelling factor for normal starch (NS) (green square), high-amylose starch (HAS) (blue triangle) and waxy starch (WS) (purple circle).

Table 4
Amount of amylose leached out (LA) in the continuous phase of 4% high-amylose starch (HAS) and normal starch (NS) samples with different gelatinization degree (GD). Waxy starch is not included as it does not contain any amylose.

HAS			NS		
GD	LA dry matter/total starch dry matter (%)	LA/total amylose content (%)	GD	LA dry matter/total starch dry matter (%)	LA/total amylose content (%)
2.4	3.4	4.8	2.2	3.6	15.6
2.7	5.0	7.1	7.4	5.4	24.4
3.2	7.4	10.5	9.1	6.8	28.9
5.9	9.6	13.6	14.6	11.4	53.1
6.2	11.8	16.9	18.2	15.8	75.4

the granules. As NS showed a higher swelling capacity, more amylose leached out considering the total amount of amylose in the granules (Table 4). In NS, 75.4% of total amylose was able to leach out of the granules, whereas in HAS this was only 16.9%. This can again be explained by the fact that HAS contained more stable crystalline structures, which required more energy to dissociate (Chen & Stokes, 2012; Cornejo-Ramírez et al., 2018; Debet & Gidley, 2006). For both NS and HAS, amylose was thus present in the continuous phase, and slightly higher values were found for NS.

3.5. Effect of continuous phase on granule lubrication

The leached-out amylose can increase the viscosity of the starch suspensions, which can consequently alter their lubrication behavior (Liu et al., 2016). To investigate the effect of amylose in the continuous phase, two NS suspensions, one with the lowest (2.5) and one with the highest SF (26.5) were selected. These suspensions also showed the largest difference in the friction behavior (Fig. 3). The friction behavior of the whole suspensions and those of the two separated phases were also evaluated (data shown in supplementary information as Fig. A.5).

In the boundary regime the friction coefficient of the leached-out amylose was approximately 0.5, which was lower than that of the granule phase in the case of limited swelling (SF = 2.5), but higher than the friction coefficient of the highly swollen granules (SF = 26.5) (data shown in supplementary information as Fig. A.5a and b). For both SF values, the friction coefficient of the whole suspension was higher than that of the granule phase. The leached-out amylose in the continuous phase thus decreased the lubrication capacity for both small stiff particles and large deformable particles. The negative effect of amylose on lubrication was also observed in other starch studies (Liu et al., 2016). In addition, for both SF values, the friction curve of the whole suspension was more similar to the one of the granule phase than that of the continuous amylose phase. These results support the hypothesis that the granule phase dominated the lubrication behavior.

The effect of amylose on the lubrication efficiency of the granules may be due to the fact that the amylose increased the viscosity of the continuous phase. The increased viscosity increased the friction between particles and inhibited the mobility of the granules, thus increasing the friction coefficient of the systems. If so, a higher amount of amylose in the continuous phase would be expected to further decrease particle lubrication, i.e. increase friction, by limiting granules sliding/rolling. To confirm this, an extra amount of amylose (up to 23.3%), which was higher than the natural concentration (15.8%), was added to the highly swollen granule phase (SF = 26.5). Due to the limited solubility of amylose obtained via freeze-drying, the maximum content of amylose in the continuous phase was 23.3%. The friction coefficient increased with an increasing amount of amylose in the continuous phase, confirming that the amylose in the continuous phase decreased the lubrication properties of the swollen granules (data shown in supplementary information as Fig. A.5c).

3.6. Effect of saliva on lubrication behavior of starch dispersions

As starch is prone to degradation by amylase present in saliva, the tribological properties of starch suspensions may change during consumption. Also, mucin and PRPs in saliva have been shown to provide good lubrication (Baum, 1993; Morell et al., 2017; Payment et al., 2000), and may thus influence the lubrication behavior of starch suspensions during oral conditions. Therefore, a series of samples with added human saliva was incorporated in this study. The composition of saliva was determined by SDS-page to confirm the presence of amylase, mucin, and proline-rich-proteins (data not shown). The degree of hydrolysis for starch suspensions was checked by incubating mixtures of saliva and starch with a saliva: starch ratio of 1:9 (w/w) under stirring (300 rpm) at 37 °C. We found that the most swollen granules (SF = 26.5) were fully hydrolyzed by saliva after 1.5 h, when no granules were present anymore in the sample. In samples with native and the less swollen granules (SF = 2.5), granules still existed after 18 h. Thus, with such a low proportion of saliva and within the short time frame of oral processing for liquid foods and that of our tribological measurements (4 min), starch granules were expected to change only to a limited extent as a result of amylase hydrolysis. In other words, we assumed the activity of amylase in saliva to have little influence on the lubrication properties of the suspensions.

We first measured the friction properties of starch suspensions and we then added saliva to evaluate the effect of saliva on starch lubrication. To illustrate the results, we take the friction coefficient of the different samples at a sliding speed of 1 mm/s. As shown in Fig. 6a, differences among the three types of native starches were observed, as expected from the previous results. Whereas the friction coefficients of NS and HAS were comparable, that of WS was much lower. The friction coefficients decreased upon the addition of saliva for all three types of native starch. Noticeably, the friction coefficients of mixtures containing saliva and starch were close to that of saliva alone, implying that saliva dominated the friction and masked the difference in starch samples regardless of starch type. The effect of dilution on the friction coefficient was checked by adding the same amount of water to the suspensions. This addition had limited influence on lubrication, indicating that the reduction in friction was caused by components present in saliva, such as salivary proteins. It has been reported that proteins in human saliva, including mucin and proline-rich-proteins (PRP-1), can adsorb on the hydrophobic PDMS surfaces and form a viscous film, providing pronounced lubricating effects (Baum, 1993; Xu, Blennow, et al., 2020; Xu, Liamas, et al., 2020). In our study, saliva components likely prevented direct contact between the particles and opposing sliding surfaces, and the decreased particle-surface contact masked the difference in moving ability of different particles, leading to similar friction coefficients.

As larger particles were able to provide better particle lubrication, we also compared the effect of saliva addition to suspensions with low and high SF (Fig. 6b). The addition of saliva decreased friction of stiff granules (SF = 2.5), but slightly increased the friction of more deformable granules (SF = 26.5). In both cases, the friction of the mixtures of saliva and swollen starch were close to that of saliva alone, indicating that saliva influenced lubrication for both native and swollen granules. Even though saliva and the amylose phase gave similar friction coefficients on their own, salivary proteins were able to reduce the friction coefficient of granules, whereas amylose did not. This may be due to the different affinity of the components of saliva and amylose for the hydrophobic PDMS surface. Amylose is a linear polymer composed of 1,4-linked D-glucose units and shows high hydrophilicity (Domene-López et al., 2019; Mua & Jackson, 1997). Amylose thus has a lower affinity to

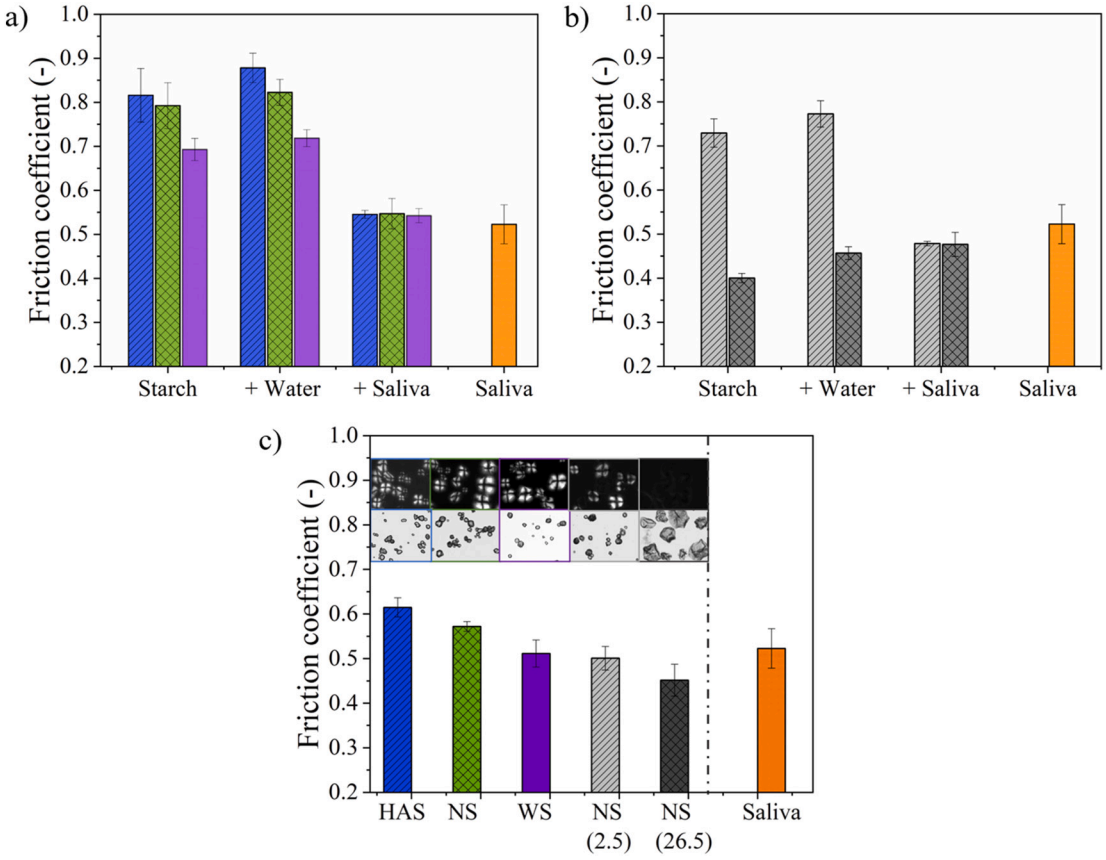

Fig. 6. Friction coefficient at a constant sliding speed of 1 mm/s of a) high-amylose starch (HAS) (blue bar with slash), normal starch (NS) (green bar with cross), waxy starch (WS) (purple bar); b) NS with a swelling factor (SF) of 2.5 (light grey bar with slash) and 26.5 (dark grey bar with cross). In both graphs saliva is present as a reference (orange bar); c) for starch samples measured on the sliding surfaces pre-adsorbed with a saliva layer. Saliva is present as a reference.

adhere to a hydrophobic PDMS and form a viscous film. In contrast, salivary proteins are amphiphilic, and can adhere to the hydrophobic PDMS through hydrophobic interaction to form a hydrated viscous film (Baum, 1993; Carpenter, 2013; Rudge et al., 2021). Thus, the film formed by salivary proteins had a far greater impact on lubrication than that of amylose.

To verify that the friction coefficients are determined by the formed salivary proteins on the PDMS surface, we performed an additional experiment. First, a layer of saliva was applied to the PDMS substrate, and then the starch suspensions were added on top of this layer. The friction coefficients of different starch suspensions can be observed in Fig. 6c. We found that the friction coefficients of the starch samples measured on a saliva pre-coated surface was lower than on a bare PDMS surface (except SF = 26.5), but also that the samples did not reach the friction coefficient of the saliva alone. These results show not only that the salivary film determined the lubrication properties, but also that the starch particles still had an effect in this case.

The salivary film alone, therefore, does not explain why the starch suspensions in Fig. 6a and b provided friction coefficients very close to that of saliva. These results suggest that not only the salivary layer, but also the salivary proteins in the bulk phase play a role in determining the friction coefficient. The salivary proteins may reduce friction and interlocking between the starch particles, or increase the gap size due to increased viscosity.

These results show that the lubrication properties of starch suspensions are very much dependent on the starch source and on the swelling properties of the starch. In the case of HAS, the limited swelling ability of the particles and the high degree of crystallinity always provides a high friction coefficient. Once particles swell, as for NS and WS, the friction coefficients decrease to a large extent. The granules therefore play an important role in the lubrication behavior. Once the granules start to disintegrate completely, the beneficial effect of the particles disappears, and the friction coefficient increases again. This was confirmed by extensively hydrolyzing the starch, which led to an increase in the friction coefficient again (data not shown). However, during consumption, differences in lubrication properties of dispersions with different starches may disappear, as both the salivary layer present on the tongue, and the saliva present as the bulk phase begin to affect lubrication.

4. Conclusion

The lubrication behavior of starch suspensions appears to be dominated by the granule properties and to be mostly influenced by the particle size, and thus the swelling factor (SF) of the granules. In our study, granules of normal maize starch with an amylose content of 25% had the highest swelling capacity, leading to the largest particle size, and thus gave the best lubrication properties. In contrast, granules with high amylose content (70%) showed the lowest swelling capacity, i.e. smallest size, and gave the highest friction coefficients. Even though waxy starch granules (with only amylopectin) extensively swelled, upon gelatinization they broke up into smaller fragments, and therefore the friction coefficients could not further decrease. Although the properties of starch had a large influence on the tribological properties, limited differences were observed when the samples mixed with saliva. This may indicate that differences in sensory perception will also be limited, and that the effect of particles properties may be negligible. However, this would need to be confirmed with a sensory study.

CRediT authorship contribution statement

Lei Ji: Investigation, Data curation, Methodology, Visualization, Writing – original draft. **He Zhang:** Investigation, Data curation. **Leonardo Cornacchia:** Writing – review & editing. **Guido Sala:** Methodology, Validation, Supervision, Writing – review & editing. **Elke Scholten:** Conceptualization, Methodology, Validation, Writing – review & editing, Supervision, Funding acquisition.

Declaration of competing interest

The authors declare that they have no known competing financial interests or personal relationships that could have appeared to influence the work reported in this paper.

Acknowledgement

The authors would like to thank China Scholarship Council (CSC) and Danone Nutricia Research (The Netherlands) for financial support. We thank Harry Baptist, Floris Gerritsen and Roy Delahaije for technical support, and Mara Wensveen for executing part of the experiments. We also thank Hilde Ruis (Danone Nutricia Research) for valuable discussions.

Appendix A. Supplementary data

Supplementary data to this article can be found online at https://doi.org/10.1016/j.carbpol.2022.119523.

References

Alazemi, A. A., Alzubi, F. G., Alhazza, A., Dysart, A., & Pol, V. G. (2020). Rheological and wettability properties of engine oil with a submicron spherical carbon particle lubricant mixture. *International Journal of Automotive Technology, 21*(6), 1475–1482. https://doi.org/10.1007/s12239-020-0139-z

Baum, B. J. (1993). Principles of saliva secretion. *Annals of the New York Academy of Sciences, 694*, 17–23. https://doi.org/10.1111/j.1749-6632.1993.tb18338.x

BeMiller, J. N. (2011). Pasting, paste, and gel properties of starch–hydrocolloid combinations. *Carbohydrate Polymers, 86*(2), 386–423. https://doi.org/10.1016/j.carbpol.2011.05.064

Bi, D., Zhang, J., Chakraborty, B., & Behringer, R. P. (2011). Jamming by shear. *Nature, 480*(7377), 355–358. https://doi.org/10.1038/nature10667

Carpenter, G., Bozorgi, S., Vladescu, S., Forte, A. E., Myant, C., Potineni, R. V., & Baier, S. K. (2019). A study of saliva lubrication using a compliant oral mimic. *Food Hydrocolloids, 92*, 10–18. https://doi.org/10.1016/j.foodhyd.2019.01.049

Carpenter, G. H. (2013). The secretion, components, and properties of saliva. *Annual Review of Food Science and Technology, 4*(1), 267–276. https://doi.org/10.1146/annurev-food-030212-182700

Cassin, G., Heinrich, E., & Spikes, H. A. (2001). The influence of surface roughness on the lubrication properties of adsorbing and non-adsorbing biopolymers. *Tribology Letters, 11*(2), 95–102. https://doi.org/10.1023/A:1016702906095

Chen, J., & Stokes, J. R. (2012). Rheology and tribology: Two distinctive regimes of food texture sensation. *Trends in Food Science & Technology, 25*(1), 4–12. https://doi.org/10.1016/j.tifs.2011.11.006

Chojnicka, A., De Jong, S., De Kruif, C. G., & Visschers, R. W. (2008). Lubrication properties of protein aggregate dispersions in a soft contact. *Journal of Agricultural and Food Chemistry, 56*(4), 1274–1282. https://doi.org/10.1021/jf0720988

Cornejo-Ramírez, Y. I., Martínez-Cruz, O., Del Toro-Sánchez, C. L., Wong-Corral, F. J., Borboa-Flores, J., & Cinco-Moroyoqui, F. J. (2018). The structural characteristics of starches and their functional properties. *CyTA - Journal of Food, 16*(1), 1003–1017. https://doi.org/10.1080/19476337.2018.1518343

de Clerck, P. (2009). Starch in the wet-end. In I. Thorn, & C. O. Au (Eds.), *Applications of wet-end paper chemistry* (pp. 171–194). Dordrecht: Springer Netherlands.

de Vicente, J., Stokes, J. R., & Spikes, H. A. (2006). Soft lubrication of model hydrocolloids. *Food Hydrocolloids, 20*(4), 483–491. https://doi.org/10.1016/j.foodhyd.2005.04.005

De Wijk, R. A., & Prinz, J. F. (2006). Mechanisms underlying the role of friction in oral texture. *Journal of Texture Studies, 37*(4), 413–427. https://doi.org/10.1111/j.1745-4603.2006.00060.x

Debet, M. R., & Gidley, M. J. (2006). Three classes of starch granule swelling: Influence of surface proteins and lipids. *Carbohydrate Polymers, 64*(3), 452–465. https://doi.org/10.1016/j.carbpol.2005.12.011

Debet, M. R., & Gidley, M. J. (2007). Why do gelatinized starch granules not dissolve completely? Roles for amylose, protein, and lipid in granule "ghost" integrity. *Journal of Agricultural and Food Chemistry, 55*(12), 4752–4760. https://doi.org/10.1021/jf070004o

Desse, M., Fraiseau, D., Mitchell, J., & Budtova, T. (2010). Individual swollen starch granules under mechanical stress: Evidence for deformation and volume loss. *Soft Matter, 6*(2), 363–369. https://doi.org/10.1039/B914911B

Domene-López, D., García-Quesada, J. C., Martin-Gullon, I., & Montalbán, M. G. (2019). Influence of starch composition and molecular weight on physicochemical properties of biodegradable films. Retrieved from *Polymers, 11*(7), 1084 https://www.mdpi.com/2073-4360/11/7/1084.

Dresselhuis, D. M., de Hoog, E. H. A., Cohen Stuart, M. A., & van Aken, G. A. (2008). Application of oral tissue in tribological measurements in an emulsion perception context. *Food Hydrocolloids, 22*(2), 323–335. https://doi.org/10.1016/j.foodhyd.2006.12.008

Fan, N., Shewan, H. M., Smyth, H. E., Yakubov, G. E., & Stokes, J. R. (2021). Dynamic tribology protocol (DTP): Response of salivary pellicle to dairy protein interactions validated against sensory perception. *Food Hydrocolloids, 113*, Article 106478. https://doi.org/10.1016/j.foodhyd.2020.106478

Gabriele, A., Spyropoulos, F., & Norton, I. T. (2010). A conceptual model for fluid gel lubrication. *Soft Matter, 6*(17), 4205–4213. https://doi.org/10.1039/C001907K

Genovese, D. B., & Rao, M. A. (2003). Role of starch granule characteristics (volume fraction, rigidity, and fractal dimension) on rheology of starch dispersions with and without amylose. *Cereal Chemistry, 80*(3), 350–355. https://doi.org/10.1094/CCHEM.2003.80.3.350

Hafez, A., Liu, Q., Finkbeiner, T., Alouhali, R. A., Moellendick, T. E., & Santamarina, J. C. (2021). The effect of particle shape on discharge and clogging. *Scientific Reports, 11*(1), 3309. https://doi.org/10.1038/s41598-021-82744-w

Hwang, Y., Lee, C., Choi, Y., Cheong, S., Kim, D., Lee, K., & Kim, S. H. (2011). Effect of the size and morphology of particles dispersed in nano-oil on friction performance between rotating discs. *Journal of Mechanical Science and Technology, 25*(11), 2853–2857. https://doi.org/10.1007/s12206-011-0724-1

Jenkins, P. J., & Donald, A. M. (1998). Gelatinisation of starch: A combined SAXS/WAXS/DSC and SANS study. *Carbohydrate Research, 308*(1), 133–147. https://doi.org/10.1016/S0008-6215(98)00079-2

Kokini, J. L., Kadane, J. B., & Cussler, E. L. (1977). Liquid texture perceived in the mouth. *Journal of Texture Studies, 8*(2), 195–218. https://doi.org/10.1111/j.1745-4603.1977.tb01175.x

Lafond, P. G., Gilmer, M. W., Koh, C. A., Sloan, E. D., Wu, D. T., & Sum, A. K. (2013). Orifice jamming of fluid-driven granular flow. *Physical Review E: Statistical, Nonlinear, and Soft Matter Physics, 87*(4), Article 042204. https://doi.org/10.1103/PhysRevE.87.042204

Liu, K., Stieger, M., van der Linden, E., & van de Velde, F. (2016). Tribological properties of rice starch in liquid and semi-solid food model systems. *Food Hydrocolloids, 58*, 184–193. https://doi.org/10.1016/j.foodhyd.2016.02.026

Lourdin, D., Putaux, J.-L., Potocki-Véronèse, G., Chevigny, C., Rolland-Sabaté, A., & Buléon, A. (2015). Crystalline structure in starch. In Y. Nakamura (Ed.), *Starch: Metabolism and structure* (pp. 61–90). Tokyo: Springer Japan.

Lund, D., & Lorenz, K. J. (1984). Influence of time, temperature, moisture, ingredients, and processing conditions on starch gelatinization. *C R C Critical Reviews in Food Science and Nutrition, 20*(4), 249–273. https://doi.org/10.1080/10408398409527391

Macakova, L., Yakubov, G. E., Plunkett, M. A., & Stokes, J. R. (2010). Influence of ionic strength changes on the structure of pre-adsorbed salivary films. A response of a natural multi-component layer. *Colloids and Surfaces B: Biointerfaces, 77*(1), 31–39. https://doi.org/10.1016/j.colsurfb.2009.12.022

Malinski, E., Daniel, J. R., Zhang, X. X., & Whistler, R. L. (2003). Isolation of small starch granules and determination of their fat mimic characteristics. *Cereal Chemistry, 80*(1), 1–4. https://doi.org/10.1094/CCHEM.2003.80.1.1

Mason, W. R. (2009). Chapter 20 - Starch use in foods. In J. BeMiller, & R. Whistler (Eds.), *Starch* (3rd ed., pp. 745–795). San Diego: Academic Press.

Morell, P., Chen, J., & Fiszman, S. (2017). The role of starch and saliva in tribology studies and the sensory perception of protein-added yogurts. *Food & Function, 8*(2), 545–553. https://doi.org/10.1039/C6FO00259E

Mua, J. P., & Jackson, D. S. (1997). Fine structure of corn amylose and amylopectin fractions with various molecular weights. *Journal of Agricultural and Food Chemistry, 45*(10), 3840–3847. https://doi.org/10.1021/jf960877a

Nguyen, P. T. M., Kravchuk, O., Bhandari, B., & Prakash, S. (2017). Effect of different hydrocolloids on texture, rheology, tribology and sensory perception of texture and mouthfeel of low-fat pot-set yoghurt. *Food Hydrocolloids, 72*, 90–104. https://doi.org/10.1016/j.foodhyd.2017.05.035

Oates, C. G. (1997). Towards an understanding of starch granule structure and hydrolysis. *Trends in Food Science & Technology, 8*(11), 375–382. https://doi.org/10.1016/S0924-2244(97)01090-X

Olivares, M. L., Shahrivar, K., & de Vicente, J. (2019). Soft lubrication characteristics of microparticulated whey proteins used as fat replacers in dairy systems. *Journal of Food Engineering, 245*, 157–165. https://doi.org/10.1016/j.jfoodeng.2018.10.015

Payment, S. A., Liu, B., Offner, G. D., Oppenheim, F. G., & Troxler, R. F. (2000). Immunoquantification of human salivary mucins MG1 and MG2 in stimulated whole saliva: Factors influencing mucin levels. *Journal of Dental Research, 79*(10), 1765–1772. https://doi.org/10.1177/00220345000790100601

Pérez, S., Baldwin, P. M., & Gallant, D. J. (2009). Chapter 5 - Structural features of starch granules I. In J. BeMiller, & R. Whistler (Eds.), *Starch* (3rd ed., pp. 149–192). San Diego: Academic Press.

Renzetti, S., van den Hoek, I. A. F., & van der Sman, R. G. M. (2021). Mechanisms controlling wheat starch gelatinization and pasting behaviour in presence of sugars and sugar replacers: Role of hydrogen bonding and plasticizer molar volume. *Food Hydrocolloids, 119*, Article 106880. https://doi.org/10.1016/j.foodhyd.2021.106880

Rudge, R. E. D., Fuhrmann, P. L., Scheermeijer, R., van der Zanden, E. M., Dijksman, J. A., & Scholten, E. (2021). A tribological approach to astringency perception and astringency prevention. *Food Hydrocolloids, 121*, Article 106951. https://doi.org/10.1016/j.foodhyd.2021.106951

Rudge, R. E. D., van de Sande, J. P. M., Dijksman, J. A., & Scholten, E. (2020). Uncovering friction dynamics using hydrogel particles as soft ball bearings. *Soft Matter, 16*(15), 3821–3831. https://doi.org/10.1039/D0SM00080A

Sarkar, A., Kanti, F., Gulotta, A., Murray, B. S., & Zhang, S. (2017). Aqueous lubrication, structure and rheological properties of whey protein microgel particles. *Langmuir, 33*(51), 14699–14708. https://doi.org/10.1021/acs.langmuir.7b03627

Shewan, H. M., Pradal, C., & Stokes, J. R. (2020). Tribology and its growing use toward the study of food oral processing and sensory perception. *Journal of Texture Studies, 51*(1), 7–22. https://doi.org/10.1111/jtxs.12452

Singh, N., Kaur, A., & Shevkani, K. (2014). Maize: Grain structure, composition, milling, and starch characteristics. In D. P. Chaudhary, S. Kumar, & S. Langyan (Eds.), *Maize: Nutrition dynamics and novel uses* (pp. 65–76). New Delhi: Springer India.

Sonne, A., Busch-Stockfisch, M., Weiss, J., & Hinrichs, J. (2014). Improved mapping of in-mouth creaminess of semi-solid dairy products by combining rheology, particle size, and tribology data. *LWT - Food Science and Technology, 59*(1), 342–347. https://doi.org/10.1016/j.lwt.2014.05.047

Stokes, J. R. (2011). Rheology of industrially relevant microgels. In *Microgel suspensions* (pp. 327–353).

Stokes, J. R., Boehm, M. W., & Baier, S. K. (2013). Oral processing, texture and mouthfeel: From rheology to tribology and beyond. *Current Opinion in Colloid & Interface Science, 18*(4), 349–359. https://doi.org/10.1016/j.cocis.2013.04.010

Stokes, J. R., Macakova, L., Chojnicka-Paszun, A., de Kruif, C. G., & de Jongh, H. H. J. (2011). Lubrication, adsorption, and rheology of aqueous polysaccharide solutions. *Langmuir, 27*(7), 3474–3484. https://doi.org/10.1021/la104040d

Stribiţcaia, E., Krop, E. M., Lewin, R., Holmes, M., & Sarkar, A. (2020). Tribology and rheology of bead-layered hydrogels: Influence of bead size on sensory perception. *Food Hydrocolloids, 104*, Article 105692. https://doi.org/10.1016/j.foodhyd.2020.105692

Tao, J., Huang, J., Yu, L., Li, Z., Liu, H., Yuan, B., & Zeng, D. (2018). A new methodology combining microscopy observation with artificial neural networks for the study of starch gelatinization. *Food Hydrocolloids, 74*, 151–158. https://doi.org/10.1016/j.foodhyd.2017.07.037

Upadhyay, R., Aktar, T., & Chen, J. (2020). Perception of creaminess in foods. *Journal of Texture Studies, 51*(3), 375–388. https://doi.org/10.1111/jtxs.12509

Vlădescu, S.-C., Bozorgi, S., Hu, S., Baier, S. K., Myant, C., Carpenter, G., & Reddyhoff, T. (2021). Effects of beverage carbonation on lubrication mechanisms and mouthfeel. *Journal of Colloid and Interface Science, 586*, 142–151. https://doi.org/10.1016/j.jcis.2020.10.079

Wang, M., Wang, D., Socolar, J., Zheng, H., & Behringer, R. (2019). Jamming by shear in a dilating granular system. *Granular Matter, 21*, 102. https://doi.org/10.1007/s10035-019-0951-1

Wang, S., & Copeland, L. (2013). Molecular disassembly of starch granules during gelatinization and its effect on starch digestibility: A review. *Food & Function, 4*(11), 1564–1580. https://doi.org/10.1039/C3FO60258C

Wu, Y. Y., Tsui, W. C., & Liu, T. C. (2007). Experimental analysis of tribological properties of lubricating oils with nanoparticle additives. *Wear, 262*(7), 819–825. https://doi.org/10.1016/j.wear.2006.08.021

Xu, F., Liamas, E., Bryant, M., Adedeji, A. F., Andablo-Reyes, E., Castronovo, M., & Sarkar, A. (2020). A self-assembled binary protein model explains high-performance salivary lubrication from macro to nanoscale. *Advanced Materials Interfaces, 7*(1), 1901549. https://doi.org/10.1002/admi.201901549

Xu, J., Blennow, A., Li, X., Chen, L., & Liu, X. (2020). Gelatinization dynamics of starch in dependence of its lamellar structure, crystalline polymorphs and amylose content. *Carbohydrate Polymers, 229*, Article 115481. https://doi.org/10.1016/j.carbpol.2019.115481

Yakubov, G. E., Branfield, T. E., Bongaerts, J. H. H., & Stokes, J. R. (2015). Tribology of particle suspensions in rolling-sliding soft contacts. *Biotribology, 3*, 1–10. https://doi.org/10.1016/j.biotri.2015.09.003

Yakubov, G. E., Zhong, L., Li, M., Boehm, M. W., Xie, F., Beattie, D. A., & Stokes, J. R. (2015). Lubrication of starch in ionic liquid–water mixtures: Soluble carbohydrate polymers form a boundary film on hydrophobic surfaces. *Carbohydrate Polymers, 133*, 507–516. https://doi.org/10.1016/j.carbpol.2015.06.087

Zhang, B., Selway, N., Shelat, K. J., Dhital, S., Stokes, J. R., & Gidley, M. J. (2017). Tribology of swollen starch granule suspensions from maize and potato. *Carbohydrate Polymers, 155*, 128–135. https://doi.org/10.1016/j.carbpol.2016.08.064

Zinoviadou, K. G., Janssen, A. M., & de Jongh, H. H. (2008). Tribological properties of neutral polysaccharide solutions under simulated oral conditions. *Journal of Food Science, 73*(2), E88–E94. https://doi.org/10.1111/j.1750-3841.2007.00649.x